4296 *Organometallics* **1999,** *18,* 4296−4303

Synthesis and Characterization of $\mathrm{OsH_2Cl[\kappa \mathit{N},\kappa \mathit{O}\text{-}(ON{=}CR_2)](P^iPr_3)_2}$ ($\mathrm{CR_2} = \overline{\mathrm{C(CH_2)_4C}}\mathrm{H_2}$, R = $\mathrm{CH_3}$): Influence of the $\mathrm{L_2}$ Ligand on the Nature of the $\mathrm{H_2}$ Unit in $\mathrm{OsH_2ClL_2(P^iPr_3)_2}$ ($\mathrm{L_2} = \mathrm{ON{=}CR_2}$, $\mathrm{NH{=}C(Ph)C_6H_4}$) Complexes

Ricardo Castarlenas,[†] Miguel A. Esteruelas,*[,†] Enrique Gutiérrez-Puebla,[‡]
Yves Jean,[§] Agustí Lledós,*[,‖] Marta Martín,[†] and Jaume Tomàs[‖]

Departamento de Química Inórganica-Instituto de Ciencia de Materiales de Aragón, Universidad de Zaragoza-CSIC, 50009 Zaragoza, Spain, Instituto de Ciencia de Materiales de Madrid, CSIC, Campus de Cantoblanco, 28049 Madrid, Spain, Laboratoire de Chimie Théorique (ESA Q8077), Bâtiment 490, Université de Paris Sud, 91405 Orsay Cedex, France, and Departament de Química, Universitat Autònoma de Barcelona, 08193 Bellaterra, Barcelona, Spain

Received June 1, 1999

The dihydride−dichloro complex $\mathrm{OsH_2Cl_2(P^iPr_3)_2}$ (**1**) reacts with cyclohexanone oxime and acetone oxime in the presence of $\mathrm{Et_3N}$ to give the dihydride derivatives $\mathrm{OsH_2Cl\{\kappa \mathit{N},\kappa \mathit{O}\text{-}[ON{=}\overline{C(CH_2)_4C}H_2]\}(P^iPr_3)_2}$ (**2**) and $\mathrm{OsH_2Cl\{\kappa \mathit{N},\kappa \mathit{O}\text{-}[ON{=}C(CH_3)_2]\}(P^iPr_3)_2}$ (**3**), respectively. The structure of **2** has been determined by X-ray diffraction. The geometry around the osmium atom can be described as a distorted pentagonal bipyramid, with the triisopropylphosphine ligands occupying two relative *trans* positions. The remaining perpendicular plane is formed by the hydride ligands, the chlorine, and the oximate group, which acts with a bite angle of 36.6(1)°. In solution the hydride ligands of **2** and **3** undergo an intramolecular thermally activated site exchange process. The activation parameters of this process are $\Delta H^\ddagger = 11.9(\pm 0.7)$ kcal mol^{-1} and $\Delta S^\ddagger = -0.5(\pm 1.4)$ cal mol^{-1} K^{-1} for **2** and $\Delta H^\ddagger = 11.7(\pm 0.8)$ kcal mol^{-1} and $\Delta S^\ddagger = -0.8(\pm 2.0)$ cal mol^{-1} K^{-1} for **3**. To understand why complexes **2** and **3** are dihyride derivatives, while the previously reported complex $\mathrm{\overline{OsCl\{NH{=}C(Ph)C}{}_6H_4\}(\eta^2\text{-}H_2)(P^iPr_3)_2}$ is an elongated dihydrogen compound, a quantitative theoretical analysis of the interaction between the $\mathrm{H_2}$ moiety and the $\mathrm{OsClL_2(PH_3)_2}$ ($\mathrm{L_2} = \mathrm{ON{=}CH_2}$, $\mathrm{NH{=}CHCH{=}CH}$) complex fragments, along the oxidative addition pathway, is also reported.

Introduction

Elongated dihydrogen complexes[1] are often seen as arrested structures at intermediate stages on the reaction path for the dihydrogen oxidative addition.[2] However, theoretical calculations[3−6] have suggested an alternative description for this class of compounds. Instead of as an intermediate species along the reaction path, they may be better described as complexes containing two hydrogen atoms moving freely in a large region of the coordination sphere of the metal. High-level ab initio calculations on the elongated dihydrogen complexes $\mathrm{[OsX(\eta^2\text{-}H_2)(NH_3)_4]^+}$ (X = $\mathrm{CH_3CO_2}$, Cl),[3] $\mathrm{[Ru(\eta^5\text{-}C_5H_5)(\eta^2\text{-}H_2)(H_2PCH_2CH_2PH_2)]^+}$,[4] *trans*-$\mathrm{[OsCl(\eta^2\text{-}H_2)(H_2PCH_2CH_2PH_2)_2]^+}$,[5] and $\mathrm{OsCl_2(\eta^2\text{-}H_2)(NH{=}CH_2)(PH_3)_2}$[6] have shown that there is a very flat energy profile for the stretch of the coordinated H−H bond: it costs less than 2 kcal mol^{-1} to stretch an H−H bond from 1.0 to 1.6 Å.

[†] Universidad de Zaragoza-CSIC.

[‡] Instituto de Ciencia de Materiales de Madrid.

[§] Université de Paris Sud.

[‖] Universitat Autònoma de Barcelona.

(1) (a) Chinn, M. S.; Heinekey, D. M. *J. Am. Chem. Soc.* **1990**, *112*, 5166. (b) Brammer, L.; Howard, J. A. K.; Johnson, O.; Koetzle, T. F.; Spencer, J. L.; Stringer, A. M. *J. Chem. Soc., Chem. Commun.* **1991**, 241. (c) Collman, J. P.; Wagenknecht, P. S.; Hembre, R. T.; Lewis, N. S. *J. Am. Chem. Soc.* **1990**, *112*, 1294. (d) Albinati, A.; Bakhmutov, V. I.; Caulton, K. G.; Clot, E.; Eckert, J.; Eisenstein, O.; Gusev, D. G.; Grushin, V. V.; Hauger, B. E.; Klooster, W. T.; Koetzle, T. F.; McMullan, R. K.; O'Loughlin, T. J.; Pélissier, M.; Ricci, J. S.; Sigalas, M. P.; Vymenits, A. B. *J. Am. Chem. Soc.* **1993**, *115*, 7300. (e) Hasegawa, T.; Li, Z.; Parkin, S.; Hope, H.; McMullan, R. K.; Koetzle, T. F.; Taube, H. *J. Am. Chem. Soc.* **1994**, *116*, 4352. (f) Klooster, W. T.; Koetzle, T. F.; Jia, G.; Fong, T. P.; Morris, R. H.; Albinati, A. *J. Am. Chem. Soc.* **1994**, *116*, 7677. (g) Maltby, P. A.; Schlaf, M.; Steinbeck, M.; Tough, A. J.; Morris, R. H.; Klooster, W. T.; Koetzle, T. F.; Srivastava, R. C. *J. Am. Chem. Soc.* **1996**, *118*, 5396. (h) Gross, L. C.; Young, D. M.; Schultz, A. J.; Girolami, G. S. *J. Chem. Soc., Dalton Trans.* **1997**, 3081.

(2) (a) Jessop, P. G.; Morris, R. H. *Coord. Chem. Rev.* **1992**, *121*, 155. (b) Heinekey, D. M.; Oldham, W. J., Jr. *Chem. Rev.* **1993**, *93*, 913.

(3) Craw, J. S.; Backsay, G. B.; Hush, N. S. *J. Am. Chem. Soc.* **1994**, *116*, 5937.

(4) Gelabert, R.; Moreno, M.; Lluch, J. M.; Lledós, A. *J. Am. Chem. Soc.* **1997**, *119*, 9840.

(5) Gelabert, R.; Moreno, M.; Lluch, J. M.; Lledós, A. *J. Am. Chem. Soc.* **1998**, *120*, 8168.

(6) Barea, G.; Esteruelas, M. A.; Lledós, A.; López, A. M.; Tolosa, J. I. *Inorg. Chem.* **1998**, *37*, 5033.

10.1021/om9904192 CCC: $18.00
Publication on Web 09/21/1999

It can be expected that this particular behavior of the H_2 moiety could be modified by subtle electronic and geometrical changes in the transition-metal fragment. Experimental[7a,b] and theoretical[7b,c] studies have shown that the dihidrogen or dihydride character of the H_2 unit is very dependent on the nature of the ligand disposed *trans* to the two hydrogen atoms. Indeed, for this type of system, the strength of the metal−hydrogen interaction and the behavior of the hydrogen atoms in solution is strongly dependent on the ligand disposed *cis* with regard to the H_2 unit, as is illustrated by the $OsH_2X\{\overline{NH{=}C(Ph)C}_6H_4\}(P^iPr_3)_2$ (X = H, Cl, Br, I) complexes.[8] In solution, the hydride ligands of the trihydride derivative undergo two thermally activated exchange processes, which occur at different rates. The faster one involves the hydride located *trans* to the phenyl group. The replacement of this hydride by chloride, bromide, and iodide produces significant disruptions in the interaction between the other two hydrogens and the osmium atom. Thus, in the halogenated compounds $\overline{OsX\{NH{=}C(Ph)C}_6H_4\}(\eta^2\text{-}H_2)(P^iPr_3)_2$ (X = Cl, Br, I), the H_2 unit forms elongated dihydrogen ligands, which in solution show restricted rotational motions.

The dihydride or elongated dihydrogen nature of the H_2 unit of these systems depends not only on the ligand located in the *cis* position but also on other factors, as revealed by the chemistry of the unsaturated six-coordinate osmium(IV) dihydride $OsH_2Cl_2(P^iPr_3)_2$ in the presence of nucleophilic reagents. Substitution of a chloride anion in this complex by $[EtOCS_2]^-$ and $[CH_3COS]^-$ produces saturated six-coordinate compounds, where a dihydride−elongated dihydrogen transformation has occurred.[9] Similarly, the addition of 2,2′-biimidazole (H_2bim) leads to the saturated cationic elongated dihydrogen $[OsCl(\eta^2\text{-}H_2)(H_2bim)(P^iPr_3)_2]Cl$, which by deprotonation of the H_2bim ligand with $NaBH_4$ yields the neutral species $Os(Hbim)Cl(\eta^2\text{-}H_2)(P^iPr_3)_2$. Addition of pyrazole to $OsH_2Cl_2(P^iPr_3)_2$ affords the *trans*-dichloro species $OsCl_2(\eta^2\text{-}H_2)(Hpz)(P^iPr_3)_2$, which is transformed into its *cis*-dichloro isomer by stirring in hexane at 60 °C.[10]

The above-mentioned dihydride−elongated dihydrogen transformations involve the electronic saturation of the osmium atom along with a rearrangement of its coordination polyhedron, which changes from square antiprism with two missing vertexes in the starting compound[11] to octahedron in the elongated dihydrogen derivatives.[9,10] However, it does not appear that there exists a direct relationship between the electronic saturation of the metallic center and the change in the coordination polyhedron. As a matter of fact, the substitution of the chloride anions of $OsH_2Cl_2(P^iPr_3)_2$ by acetate affords the saturated seven-coordinate osmium(IV)−dihydride complexes $OsH_2Cl(\kappa^2\text{-}O_2CCH_3)(P^iPr_3)_2$ and $OsH_2\{\kappa^1\text{-}OC(O)CH_3\}(\kappa^2\text{-}O_2CCH_3)(P^iPr_3)_2$, which in the solid state have structures similar to that of the starting material that can be also described as square antiprisms but with only one missing vertex.[12]

Scheme 1

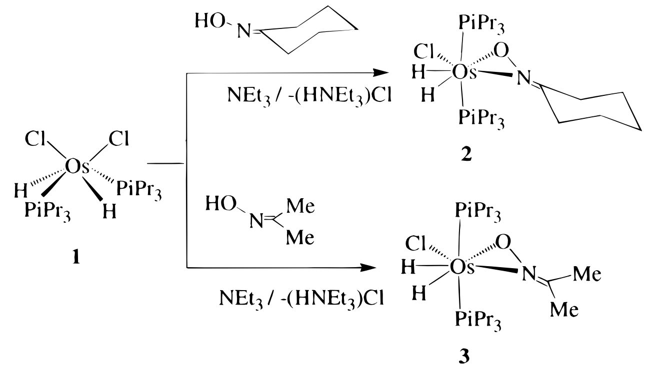

In this paper, we report the synthesis and characterization of the saturated compounds $OsH_2Cl\{\kappa N,\kappa O\text{-}(ON{=}CR_2)\}(P^iPr_3)_2$ (CR_2 = $\overline{C(CH_2)_4C}H_2$, R = CH_3). Despite having a structure similar to that of the previously mentioned elongated dihydrogen complex $\overline{OsCl\{NH{=}C(Ph)C}_6H_4\}(\eta^2\text{-}H_2)(P^iPr_3)_2$,[8] these complexes turn out to be dihydride derivatives. To understand the different natures of both types of complexes, we present also a quantitative theoretical analysis of the interaction between dihydrogen and $OsClL_2(PH_3)_2$ (L_2 = ON=CH_2, NH=CHCH=CH) complex fragments along the oxidative addition pathway.

Results and Discussion

1. Synthesis and Characterization of $OsH_2Cl\{\kappa N,\kappa O\text{-}(ON{=}CR_2)\}(P^iPr_3)_2$. Treatment at room temperature of $OsH_2Cl_2(P^iPr_3)_2$ (**1**) with the stoichiometric amount of cyclohexanone oxime or, alternatively, acetone oxime, in the presence of 5 equiv of Et_3N, gives the complexes $OsH_2Cl\{\kappa N,\kappa O\text{-}[ON{=}\overline{C(CH_2)_4C}H_2]\}(P^iPr_3)_2$ (**2**) and $OsH_2Cl\{\kappa N,\kappa O\text{-}[ON{=}C(CH_3)_2]\}(P^iPr_3)_2$ (**3**), respectively, which were isolated as yellow (**2**) and orange (**3**) solids in 82% (**2**) and 86% (**3**) yields, according to Scheme 1.

Complexes **2** and **3** were characterized by MS, elemental analysis, and IR and ^1H, $^{31}P\{^1H\}$, and $^{13}C\{^1H\}$ NMR spectroscopy. Complex **2** was further characterized by an X-ray crystallographic study. A view of the molecular geometry of this compound is shown in Figure 1. Selected bond distances and angles are listed in Table 1.

The hydrogen atoms H(1) and H(2) were located in the difference Fourier maps and refined as isotropic atoms together with the rest of the non-hydrogen atoms of the structure, giving Os−H(1) and Os−H(2) distances of 1.68(5) and 1.57(5) Å, respectively, and a H(1)−H(2) separation of 1.77(7) Å. These values suggest that the H_2 unit gives rise to two hydride ligands. In agreement with this, the IR spectra of **2** and **3** show two absorptions

---

(7) (a) Li, Z.-W.; Taube, H. *J. Am. Chem. Soc.* **1991**, *113*, 8946. (b) Bautistas, M. T.; Cappellani, E. P.; Drouin, S. D.; Morris, R. H.; Schweitzer, C. T.; Sella, A.; Zubkowski, J. *J. Am. Chem. Soc.* **1991**, *113*, 4876. (c) Craw, J. S.; Bacskay, G. B.; Hush, N. S. *J. Am. Chem. Soc.* **1994**, *116*, 5937. (d) Dapprich, S.; Frenking, G. *Organometallics* **1996**, *15*, 4547.

(8) Barea, G.; Esteruelas, M. A.; Lledós, A.; López, A. M.; Oñate, E.; Tolosa, J. I. *Organometallics* **1998**, *17*, 4065.

(9) Esteruelas, M. A.; Oro, L. A.; Ruiz, N. *Inorg. Chem.* **1993**, *32*, 3793.

(10) Esteruelas, M. A.; Lahoz, F. J.; Oro, L. A.; Oñate, E.; Ruiz, N. *Inorg. Chem.* **1994**, *33*, 787.

(11) Aracama, M.; Esteruelas, M. A.; Lahoz, F. J.; López, J. A.; Meyer, U.; Oro, L. A.; Werner, H. *Inorg. Chem.* **1991**, *30*, 288.

(12) Crochet, P.; Esteruelas, M. A.; López, A. M.; Martínez, M.-P.; Oliván, M.; Oñate, E.; Ruiz, N. *Organometallics* **1998**, *17*, 4500.

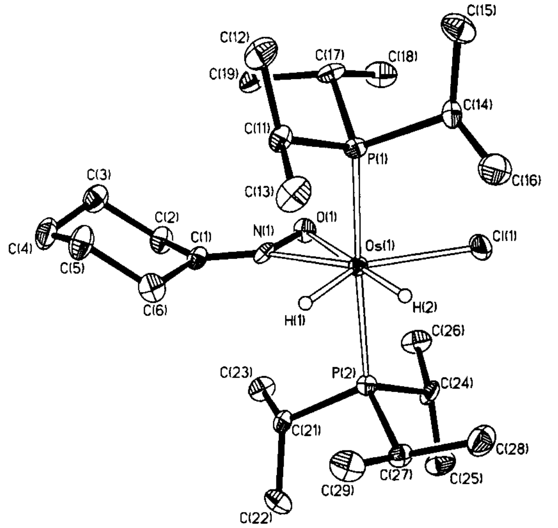

Figure 1. Molecular diagram for $OsH_2Cl\{\kappa N,\kappa O\text{-}[ON{=}\overline{C(CH_2)_4C}H_2]\}(P^iPr_3)_2$ (**2**). Thermal ellipsoids are shown at 50% probability.

Table 1. Selected Bond Lengths (Å) and Angles (deg) of $OsH_2Cl\{\kappa N,\kappa O\text{-}[ON{=}\overline{C(CH_2)_4C}H_2]\}(P^iPr_3)_2$ (2) and B3LYP Optimized Parameters of $OsH_2Cl[\kappa N,\kappa O\text{-}(O{=}NCH_2)](PH_3)_2$ (4)

	2	4		2	4
Os−Cl	2.3922(12)	2.438	P(2)−Os−O	93.04(8)	91.8
Os−P(1)	2.3798(11)	2.349	P(1)−Os−N	93.51(10)	92.2
Os−P(2)	2.3767(12)	2.349	P(1)−Os−H(1)	90(2)	90.3
Os−O	2.250(4)	2.321	P(1)−Os−H(2)	87.1(14)	88.3
Os−N	1.978(4)	2.014	P(2)−Os−N	92.55(11)	92.2
Os−H(1)	1.68(5)	1.610	P(2)−Os−H(1)	84.6(14)	90.3
Os−H(2)	1.57(5)	1.610	P(2)−Os−H(2)	85(1)	88.3
O−N	1.353(4)	1.296	O−N−C(1)	124.3(4)	126.7
N−C(1)	1.281(6)	1.291	O−Os−N	36.61(12)	33.9
Cl−Os−P(1)	90.16(4)	88.4	O−Os−H(1)	118.2(2)	115.6
Cl−Os−P(2)	89.39(4)	88.4	O−Os−H(2)	175(2)	178.5
Cl−Os−O	100.69(8)	101.7	H(1)−Os−H(2)	66(2)	62.9
Cl−Os−N	137.30(10)	135.6	Os−N−C(1)	152.9(3)	147.2
Cl−Os−H(1)	141(2)	142.6	Os−O−N	60.7(2)	60.0
Cl−Os−H(2)	75.3(14)	79.7	Os−N−O	82.7(2)	86.1
P(1)−Os−P(2)	171.53(4)	175.7	N−Os−H(1)	82(2)	81.7
P(1)−Os−O	95.35(8)	91.8	N−Os−H(2)	147.4(14)	144.6

at 2220 and 2157 cm^{-1} (**2**) and 2189 and 2165 cm^{-1} (**3**) corresponding to the ν(Os−H) vibrations, while absorptions in the typical region of dihydrogen ligands (3100−2400 cm^{-1})[2a] are not observed.

In general, the M−H distances obtained from X-ray diffraction data are imprecise.[13] However, ab initio calculations have been shown to provide useful accurate data for the hydrogen positions in both classical polyhydride[14] and dihydrogen complexes.[15] Therefore, to corroborate the dihydride nature of the H_2 unit of these compounds, a B3LYP geometry optimization was performed on the $OsH_2Cl\{\kappa N,\kappa O\text{-}(ON{=}CH_2)\}(PH_3)_2$ (**4**) model system. The structure obtained in this way is shown in Figure 2a, and the main geometrical parameters are collected in Table 1.

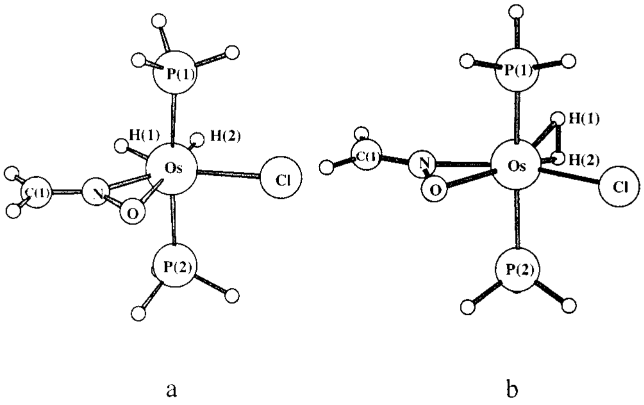

Figure 2. B3LYP optimized structures of the minimum **4** (a) and the transition state **4**-TS (b).

The theoretical results agree well with those obtained from the X-ray diffraction experiment. The Os−H (1.610 Å) distances and the H(1)−H(2) separation (1.680 Å) are statistically identical with those experimentally obtained and corroborate the dihydride nature of the H_2 unit in these compounds.

Assuming that the H_2 and the $ON{=}CR_2$ units both occupy two sites in the coordination sphere of the metal, the geometry around the osmium atom of **2** can be rationalized as a very distorted pentagonal bipyramid with the two phosphorus atoms of the triisopropylphosphine ligands occupying axial positions (P(1)−Os−P(2) = 171.53(4)°) and the hydrides, the chlorine, and the oximate group located in the equatorial plane. The distortion of the coordination polyhedron is mainly due to the oximate group, which acts with a bite angle of 36.61(12)°. Similar values have been found in related compounds.[16] If the oximate group is considered as a monodentate ligand, the structure of the complex can be described as a slightly distorted octahedron.

In agreement with the structure shown in Figure 1, the $^{31}P\{^1H\}$ NMR spectrum of **2** contains a singlet at 12.3 ppm. In the $^{13}C\{^1H\}$ NMR spectrum, the most noticeable resonance is a singlet at 139.4 ppm, corresponding to the C=N carbon atom of the oximate ligand.

---

[13] Zhao, D.; Bau, R. *Inorg. Chim. Acta* **1998**, *269*, 162.

[14] (a) Lin, Z.; Hall, M. B. *Inorg. Chem.* **1991**, *30*, 2569. (b) Lin, Z.; Hall, M. B. *Coord. Chem. Rev.* **1994**, *135*, 845. (c) Esteruelas, M. A.; Jean, Y.; Lledós, A.; Oro, L. A.; Ruiz, N.; Volatron, F. *Inorg. Chem.* **1994**, *33*, 3609. (d) Buil, M. L.; Espinet, P.; Esteruelas, M. A.; Lahoz, F. J.; Lledós, A.; Martínez-Ilarduya, J. M.; Maseras, F.; Modrego, J.; Oñate, E.; Oro, L. A.; Sola, E.; Valero, C. *Inorg. Chem.* **1996**, *35*, 1250. (e) Camanyes, S.; Maseras, F.; Moreno, M.; Lledós A.; Lluch, J. M.; Bertrán, J. *J. Am. Chem. Soc.* **1996**, *118*, 4617. (f) Demachy, I.; Esteruelas, M. A.; Jean, Y.; Lledós, A.; Maseras, F.; Oro, L. A.; Valero, C.; Volatron, F. *J. Am. Chem. Soc.* **1996**, *118*, 8388. (g) Castillo, A.; Barea, G.; Esteruelas, M. A.; Lahoz, F. J.; Lledós, A.; Maseras, F.; Modrego, J.; Oñate, E.; Oro, L. A.; Ruiz, N.; Sola, E. *Inorg. Chem.* **1999**, *38*, 1814. (h) Buil, M. L.; Esteruelas, M. A.; Modrego, J.; Oñate, E. *New J. Chem* **1999**, *23*, 403.

[15] (a) Dapprich, S.; Frenking, G. *Angew. Chem., Int. Ed. Engl.* **1995**, *24*, 354. (b) Bakhmutov, V. I.; Bertrán, J.; Esteruelas, M. A.; Lledós, A.; Maseras, F.; Modrego, J.; Oro, L. A.; Sola, E. *Chem. Eur. J.* **1996**, *2*, 1815. (c) Maseras, F.; Lledós, A.; Costas, M.; Poblet, J. M. *Organometallics* **1996**, *15*, 2947. (d) Gelabert, R.; Moreno, M.; Lluch, J. M.; Lledós, A. *Organometallics* **1997**, *16*, 3805. (e) Albéniz, M. J.; Esteruelas, M. A.; Lledós, A.; Maseras, F.; Oñate, E.; Oro, L. A.; Sola, E.; Zeier, B. *J. Chem. Soc., Dalton Trans.* **1997**, 181.

[16] (a) Dickman, M. H.; Doedens, R. J. *Inorg. Chem.* **1982**, *21*, 682. (b) Porter, L. C.; Doedens, R. J. *Acta Crystallogr., Sect. C* **1985**, *41*, 838. (c) Jaitner, P.; Huber, W.; Gieren, A.; Betz, H. *J. Organomet. Chem.* **1986**, *311*, 379. (d) Pizzotti, M.; Porta, F.; Cenini, S.; Demartin, F.; Masciocchi, N. *J. Organomet. Chem.* **1987**, *330*, 265. (e) Stella, S.; Floriani, C.; Chiesi-Villa, A.; Guastini, C. *J. Chem. Soc., Dalton Trans.* **1988**, 545. (f) Sharp, P. R.; Hoard, D. W.; Barnes, C. L. *J. Am. Chem. Soc.* **1990**, *112*, 2024. (g) Hoard, D. W.; Sharp, P. R. *Inorg. Chem.* **1993**, *32*, 612. (h) Ang, H. G.; Kwik, W. L.; Ong, K. K. *J. Fluorine Chem.* **1993**, *60*, 43. (i) Vogel, S.; Huttner, G.; Zsolnai, L.; Emmerich, C. *Z. Naturforsch., B* **1993**, *48*, 353. (j) Werner, H.; Daniel, T.; Knaup, W.; Nürnberg, O. *J. Organomet. Chem.* **1993**, *462*, 309. (k) Skoog, S. J.; Campbell, J. P.; Gladfelter, W. L. *Organometallics* **1994**, *13*, 4137. (l) Kukushkin, V. Y.; Tudela, D.; Pombeiro, A. J. L. *Coord. Chem. Rev.* **1996**, *156*, 333. (m) Skoog, S. J.; Gladfelter, W. L. *J. Am. Chem. Soc.* **1997**, *119*, 11049.

The $^{31}P\{^1H\}$ and $^{13}C\{^1H\}$ NMR spectra are temperature-invariant. However, the ^1H NMR spectrum is temperature-dependent. At 373 K in toluene-d_8 as solvent, the spectrum shows in the hydride region a broad resonance centered at −7.83 ppm. Between 323 and 293 K decoalescence occurs, and between 263 and 233 K, two signals centered at −3.22 and −12.44 ppm are observed.

The NMR spectroscopic data of **3** agree well with those of **2**. The $^{31}P\{^1H\}$ NMR spectrum shows a singlet at 12.4 ppm, and the $^{13}C\{^1H\}$ NMR spectrum contains a singlet at 133.9 ppm corresponding to the C=N carbon atom of the oximate group. As for **2**, these spectra are temperature-invariant, while the ^1H NMR spectrum is temperature-dependent. The variation of the hydride resonances with the temperature is similar to the case of **2**. At 373 K in toluene-d_8 as solvent, the spectrum shows at −7.70 ppm a broad resonance. Between 313 and 273 K, decoalescence occurs, and between 273 and 233 K, two signals centered at −3.24 and −12.60 ppm are observed.

To estimate the hydrogen−hydrogen separation between the hydride ligands of **2** and **3** in solution, the T_1 values of the hydride resonances were determined over the temperature range 253−193 K. The same T_1(min) value was found for both compounds and for each resonance (100 (±3) ms), and it occurs at the same temperature (213 K). The total relaxation rate for H_n ($R_n = 1/T_1(\text{min})(H_n)$) is the addition of the relaxation rate due to the dipole−dipole interaction (R_{H-H}) and that due to all other relaxation contributors (R^*). Since the latter one has been estimated as 5.2 s^{-1},[17] we can determine that the relaxation rate due to the hydride−hydride interaction is 4.8 s^{-1}. Using the standard equation,[18] this value leads to a separation between the hydride ligands of **2** and **3** of 1.7 Å, which agrees well with those determined by X-ray diffraction (1.77(7) Å) and theoretical methods (1.680 Å).

The behavior of the ^1H NMR spectra of **2** and **3** with changes in the temperature indicates that the hydride ligands of these compounds undergo a thermally activated site exchange process. Line-shape analysis of the $^1H\{^{31}P\}$ NMR spectra (Figure 3 shows those of **2**) allows the calculation of the rate constants for the processes at each temperature (Table 2). The activation parameters obtained from the corresponding Eyring analysis are $\Delta H^{\ddagger} = 11.9(\pm 0.7)$ kcal mol^{-1} and $\Delta S^{\ddagger} = -0.5(\pm 1.4)$ cal mol^{-1} K^{-1} for **2** and $\Delta H^{\ddagger} = 11.7(\pm 0.8)$ kcal mol^{-1} and $\Delta S^{\ddagger} = -0.8(\pm 2.0)$ cal mol^{-1} K^{-1} for **3**. The values for the entropy activation, close to zero, are in agreement with an intramolecular process, while the values for the enthalpy of activation lie in the range reported for thermal exchange processes in trihydride and hydride−dihydrogen derivatives.[20]

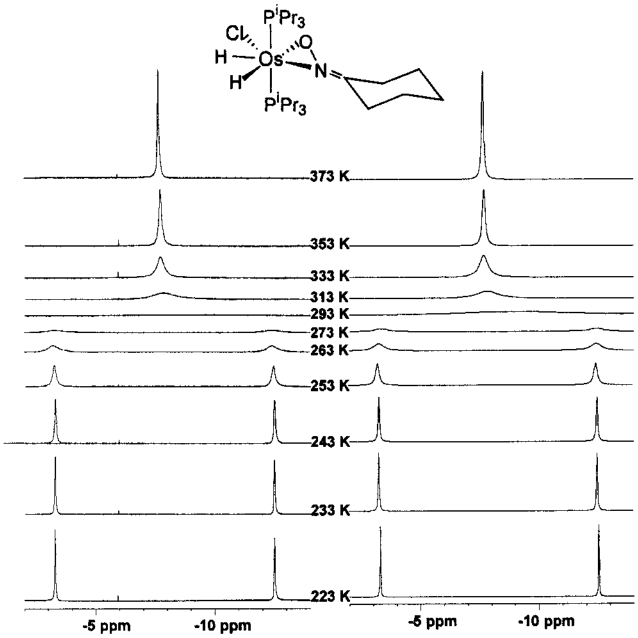

Figure 3. Experimental (left) and calculated (right) variable-temperature 300 MHz $^1H\{^{31}P\}$ NMR spectra in the high-field region of $OsH_2Cl\{\kappa N,\kappa O\text{-}[ON{=}\overline{C(CH_2)_4CH_2}]\}(P^iPr_3)_2$ (**2**) in toluene-d_8.

Table 2. Rate Constants of Dihydride Exchange of 2 and 3

	rate (s^{-1})			rate (s^{-1})	
T (K)	**2**	**3**	*T* (K)	**2**	**3**
373	4.53 × 10^5	4.88 × 10^5	263	4.95 × 10^2	3.87 × 10^2
353	2.95 × 10^5	2.27 × 10^5	253	1.46 × 10^2	2.02 × 10^2
333	9.40 × 10^4	1.67 × 10^5	243	47.3	1.17 × 10^2
313	3.51 × 10^4	3.75 × 10^4	233	36.0	43.8
293	5.85 × 10^3	9.93 × 10^3	223	9.37	
273	6.20 × 10^2	1.96 × 10^3			

To clarify the mechanism of the hydride site exchange in **2** and **3**, we have calculated the transition state assuming a structure in which the H_2 unit is rotated by 90° with respect to its position in the minimum. The B3LYP optimized structure found in this way (**4**-TS) is shown in Figure 2b. This transition state has a η^2-H_2 nature, as is proved by the H(1)−H(2) distance and H(1)−Os−H(2) angle (0.932 Å and 32.0°, respectively). The decrease of the distance between the two exchanging hydrides is concomitant with the increase of the Os−H distances (1.690 Å). Thus, the transition state can be described as a d^6 six-coordinate Os(II) species containing a dihydrogen *trans* to the oxygen atom of the oximate ligand. Furthermore, a dramatic shortening of the Os−O distance occurs in the rotated structure (2.321 Å in **4** vs 2.170 Å in **4**-TS).

The mechanism of the hydride site exchange can be described as a pairwise exchange through a η^2-H_2 structure and involves only minor motion of the other ligands. Such a mechanism has already been shown to be operative in trihydride complexes.[6−13,14e−g] The calculated activation barrier for the hydride exchange process in **4** is 19.1 kcal mol^{-1}, a value higher than that obtained by NMR spectroscopy in **2** and **3**. This discrepancy may be due to the replacement of the bulky P^{i}Pr$_3$ and ON=CR$_2$ ($CR_2 = \overline{C(CH_2)_4CH_2}$, R = CH_3) ligands by PH_3 and ON=CH_2.

---

[17] Castillo, A.; Esteruelas, M. A.; Oñate, E.; Ruiz, N. *J. Am. Chem. Soc.* **1997**, *119*, 9691.

[18] At 300 MHz, $R_{H-H} = 129.18/r^6$.[19]

[19] (a) Hamilton, D. G.; Crabtree, R. H. *J. Am. Chem. Soc.* **1988**, *110*, 4126. (b) Bautista, M. T.; Earl, K. A.; Maltby, P. A.; Morris, R. H.; Schweitzer, C. T.; Sella, A. *J. Am. Chem. Soc.* **1988**, *110*, 7031. (c) Desrosiers, P. J.; Cai, L.; Lin, Z.; Richards, R.; Halpern, J. *J. Am. Chem. Soc.* **1991**, *113*, 4173. (d) Gusev, D. G.; Kuhlman, R.; Sini, G.; Eisenstein, O.; Caulton, K. G. *J. Am. Chem. Soc.* **1994**, *116*, 2685.

[20] (a) Earl, K. A.; Jia, G.; Maltby, P. A.; Morris, R. H. *J. Am. Chem. Soc.* **1991**, *113*, 3027. (b) Jia, G.; Drouin, S. D.; Jessop, P. G.; Lough, A. J.; Morris, R. H. *Organometallics* **1993**, *12*, 906. (c) Esteruelas, M. A.; Lahoz, F. J.; López, A. M.; Oñate, E.; Oro, L. A.; Ruiz, N.; Sola, E.; Tolosa, J. I. *Inorg. Chem.* **1996**, *35*, 7811.

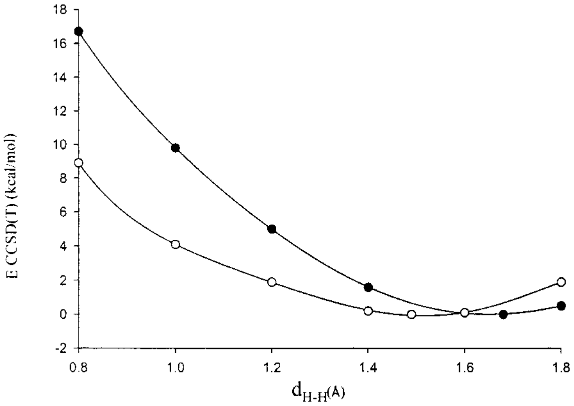

Figure 4. CCSD(T)//B3LYP potential energy curves for the H−H stretching in **4** (●) and **5** (○).

2. Analysis of the Os−H_2 Interaction. In complexes **2** and **3** the H_2 unit gives rise to two hydride ligands, whereas in the related $OsCl\{NH{=}C(Ph)C_6H_4\}(\eta^2\text{-}H_2)(P^iPr_3)_2$ it forms an elongated dihydrogen ligand.[8] Therefore, a fine balance between the different coordination modes of the H_2 moiety can be obtained just operating upon the choice of the ancillary ligands of the system.

For comparative purposes, geometry optimization of $OsCl(NH{=}CHCH{=}CH)(\eta^2\text{-}H_2)(PH_3)_2$ (**5**), taken as a model of the $OsCl\{NH{=}C(Ph)C_6H_4\}(\eta^2\text{-}H_2)(P^iPr_3)_2$ complex, was performed at the same level of theory as that used for **4**. The optimized H(1)−H(2) distance in **5** (1.494 Å) agrees with the previously calculated H−H distance in $OsCl(NH{=}CHC_6H_4)(\eta^2\text{-}H_2)(PH_3)_2$ (1.483 Å),[8] suggesting that complex **5** should be included within the rather diffuse family of elongated dihydrogen complexes.

The different natures of complexes **4** and **5** were studied by computing the energy profiles associated with the H−H bond breaking. In both complexes the H−H distance was varied from 0.8 to 1.8 Å by steps of 0.2 Å, and all the other geometrical parameters were optimized at the B3LYP level for each fixed H−H distance. Single-point energy-only calculations were performed at the CCSD(T) level on all the optimized structures. The CCSD(T)//B3LYP potential energy curves are shown in Figure 4.

In both cases there is only one minimum, and the dihydrogen form is not available. However, as expected, the minimum of **4** is slightly shifted to the dihydride region (long H−H distances). More remarkable is the fact that the shape of the two curves is clearly different. The flatness of the curve associated with the elongated dihydrogen complex **5** in the 1.2−1.8 Å region suggests that, with the inclusion of zero-point energy, the two hydrogen atoms are delocalized to a certain extent. Such a phenomenon is usual for this kind of complex,[3−6] and to give an accurate theoretical prediction of the actual H−H distance which could be obtained via neutron diffraction is not so easy. As shown previously, electronic structure calculations are not sufficient to reproduce the experimental values; nuclear wave function calculations are required.[4,5] Things are much easier for complex **4**, which is unambiguously a classical dihydride without H−H interaction. From these results, it is clear that the H_2 moiety interacts in different ways with the metal in complexes **4** and **5**. To clarify this point, a previously successfully used energy decomposition scheme[6,21] can be applied to this case. In this scheme the $OsClH_2L_2(PH_3)_2$ complexes are ideally thought to be built from two separate fragments (the H_2 molecule and the $OsClL_2(PH_3)_2$ metallic units). In this way, the interaction energy between the two fragments can be decomposed at each hydrogen−hydrogen distance into three terms. Two of them, which are unfavorable, represent the energy required to distort both fragments from their isolated equilibrium geometries to the geometry they have at each point of the curve ($\Delta E_{stretch}$ (H_2) and ΔE_{def}($OsClL_2(PH_3)_2$)). The third term is the energy gain arising from the interaction between the two distorted fragments to restore the whole complex (ΔE_{int}). At each point, the variation in the total energy (ΔE_{tot}) can be obtained according to eq 1. The results of this analysis

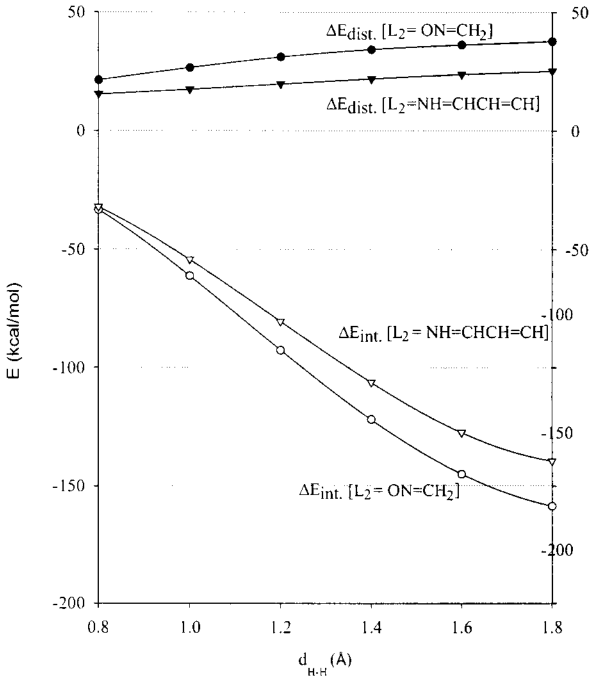

Figure 5. Energy decomposition as a function of the H−H distance for the $OsH_2Cl\{\kappa N,\kappa O\text{-}(ON{=}CH_2)\}(PH_3)_2$ (**4**) and $OsCl(NH{=}CHCH{=}CH)(\eta^2\text{-}H_2)(PH_3)_2$ (**5**) model complexes.

$$\Delta E_{tot} = \Delta E_{stretch}(H_2) + \Delta E_{def}(OsClL_2(PH_3)_2) + \Delta E_{int} \quad (1)$$

at the B3LYP level of theory are shown in Figure 5. Because we want to establish the differences between **4** and **5**, the $\Delta E_{stretch}$ (H_2) term has been omitted in this figure.

The distortion term (ΔE_{def}($OsClL_2(PH_3)_2$)) increases along the dihydrogen addition path for both complexes, since it is obviously more difficult to accommodate an elongated H_2 moiety than a dihydrogen molecule in the coordination sphere of the metal. The distortion term is larger for **4** than for **5**, because the isolated $OsClL_2(PH_3)_2$ optimized fragment is further from the geometry it has in the final structure, in the case of the ON=CH_2 ligand. However, this is not the reason for the different

---

[21] Tomàs, J.; Lledós, A.; Jean, Y. *Organometallics* **1998**, *17*, 4932.

Table 3. Energetical Parameters Related to H−H Coordination for $OsClH_2L_2(PH_3)_2$ Complexes[a]

	L_2	
	ON=CH$_2$	NH=CHCH=CH
$D_e(M-H_2)$	14.3	19.5
$\Delta E_{S/T}$	26.7	34.9
$D_e(M-H)$	81.5	83.6

[a] All the energies (in kcal/mol) have been calculated at the CCSD(T) level of theory on B3LYP optimized structures.

natures of the H_2 unit in **4** and **5**. In fact, since the slope of $\Delta E_{def}(OsClL_2(PH_3)_2)$ is slightly larger for **4** than for **5**, one should expect a dihydride form more destabilized for **4** than for **5**, and this is not observed. Thus, the understanding of the results comes from the interaction term. This term reveals that the interaction of the H_2 moiety with the complex fragment is stronger in complex **4** than in complex **5**. Furthermore, with the H−H lengthening, this difference increases, compensating the unfavorable trend found for complex **4** in the distortion term. From the curves it can also be stated that in the short H−H distances region the interaction term is too weak to allow the possibility of a dihydrogen minimum in this particular system.

3. Ability of $OsClL_2(P^iPr_3)_2$ (L_2 = ON=CR$_2$, NH=C(Ph)C_6H_4) Complex Fragments To Break the H−H Bond. In a previous work we have shown that the nature of the product of dihydrogen addition to $M(CO)_n(PH_3)_{5-n}$ (M = Cr, Mo, W; n = 0, 3, 5) can be related to the energetics of the M−H_2 and M−H bonds and to the singlet−triplet separation ($\Delta E_{S/T}$) in the ML_5 complex fragment. Dihydride structures are favored by a small singlet/triplet separation and by large M−H bonding energies ($D_e(M-H)$). We will now use this analysis to compare the complexes **4** and **5**.

The $\Delta E_{S/T}$, $D_e(M-H_2)$, and $D_e(M-H)$ terms were calculated at the CCSD(T)//B3LYP level for both complexes. With regard to the $\Delta E_{S/T}$ term it should be noted that the excitation involves the orbitals required for the further formation of the M−H bonds. The M−H_2 bond energies were calculated as the energy difference between the $OsClL_2(PH_3)_2$ fragments optimized in their lowest singlet state plus a dihydrogen molecule, and the η^2-H_2 complexes optimized with the H−H distance hold fixed to 0.8 Å. Finally, the $D_e(M-H)$ values were calculated as the energy difference between the $OsClL_2(PH_3)_2$ fragments optimized in their triplet state plus two hydrogen atoms and a structure which was the actual dihydride minimum for complex **4**, while for complex **5,** a hypothetical structure with the H−H distance fixed at 1.8 Å was taken as the dihydride. The results are collected in Table 3.

The computed values of $D_e(Os-H_2)$ are in the range of the binding energies of dihydrogen ligands in stable dihydrogen complexes (15−20 kcal mol^{-1}).[21] Thus, this magnitude by itself cannot explain why a dihydrogen structure is not found in these systems. The potential energy curves depicted in Figures 4 and 5 give a better insight into this fact: there is no energetic barrier in the H−H stretching process, so that the H−H bond breaking is not arrested at this stage. It must be stressed that the dihydrogen binding energy is higher in **5** than in **4**, indicating that at the initial stage of the oxidative addition, the Os−H_2 bond is stronger in the former. This factor works in favor of a shorter H−H equilibrium distance in complex **5**, as it was actually found in our geometry optimizations.

Experimental values of Os−H binding energies between 63 and 73 kcal mol^{-1} have been recently reported in a series of $[CpOsHL]^+$ compounds.[22a] The computed values of $D_e(Os-H)$ in **4** and **5** are 10 kcal mol^{-1} higher and similar to those determined in $[OsH(\eta^2\text{-}H_2)L_2]^+$ (L = depe, 76 kcal mol^{-1}; L = dppe, 80 kcal mol^{-1}; L = dtfpe, 81 kcal mol^{-1}).[22b] They can be placed among the strongest reported values for M−H bonds.[22c] However, this term cannot account for the different behavior of **4** and **5**: the $D_e(Os-H)$ values are very similar in both complexes. As we have found in our previous work on Kubas-like complexes,[21] the M−H binding energy depends mainly on the metal atom and remains almost unaffected by changes in the ligand (the slight difference should even favor the dihydride form in complex **5**). It is thus clear that the different behavior toward the H_2 coordination of the $OsCl_2L_2(PH_3)_2$ complex fragments is related to the $\Delta E_{S/T}$ term. All other things being equal, the smaller singlet−triplet energy promotion gives rise to the easier formation of the dihydride form. The singlet/triplet gap is lower for L_2 = ON=CH$_2$ than for L_2 = NH=CHCH=CH (26.7 vs 34.9 kcal mol^{-1}), making the dihydride formation easier in the former. This difference in the $\Delta E_{S/T}$ can be understood by taking into account the structural differences between the two types of complex fragments. NH=CHCH=CH is a bidentate ligand with a bite angle of 75°. It occupies two sites in the coordination sphere of the metal, and the corresponding complex fragment can be described as a d^6 ML_5 distorted-square-pyramidal system. The N−Os−Cl and C−Os−Cl angles (117 and 167°, respectively) agree with this description. On the other hand, the ON=CR$_2$ ligands have a bite angle of about 37°, making the OsCl(ON=CR$_2$)(PR$_3$)$_2$ fragment better described as a square-planar d^6 ML_4 system, with N−Os−Cl and O−Os−Cl angles of about 157 and 166°, respectively. Since the HOMO/LUMO gap is lower in a square-planar d^6 ML_4 fragment than in a square-pyramidal d^6 ML_5 fragment, the observed trend found for the singlet−triplet energy separation can be easily rationalized on orbital grounds.

Concluding Remarks

We have previously shown that the H_2 moiety of the complex OsCl{NH=C(Ph)C_6H_4}(η^2-H_2)(P^iPr_3)$_2$ forms an elongated dihydrogen ligand. This study reveals that a fine balance between different coordination modes of the H_2 moiety in $OsClH_2L_2(P^iPr_3)_2$ systems can be obtained just operating upon the choice of the L_2 ancillary ligands. Thus, we now show that in the presence of Et_3N the dihydride−dichloro complex $OsH_2Cl_2(P^iPr_3)_2$ reacts with oximes to give the related compounds OsH_2Cl-{κN,κO-(ON=CR$_2$)}(P^iPr_3)$_2$, where, in contrast to OsCl-{NH=C(Ph)C_6H_4}(η^2-H_2)(P^iPr_3)$_2$, the H_2 moiety gives rise to two hydride ligands.

Theoretical calculations suggest that the interaction of the H_2 moiety with the OsCl{κN,κO-(ON=CR$_2$)}-

---

(22) (a) Cappellani, E. P.; Drouin, S. D.; Jia, G.; Maltby, P. A.; Morris, R. H.; Schweitzer, C. T. *J. Am. Chem. Soc.* **1994**, *116*, 3375. (b) Wang, D.; Angelici, R. J. *J. Am. Chem. Soc.* **1996**, *118*, 935. (c) Martinho Simões, J. A.; Beauchamp, J. L. *Chem. Rev.* **1990**, *90*, 629 and references therein.

$(P^iPr_3)_2$ complex fragments is stronger than that with $OsCl\{NH{=}C(Ph)C_6H_4\}(P^iPr_3)_2$. Moreover, in agreement with the experimental results, the interaction of the H_2 moiety with the model system $OsCl\{\kappa N,\kappa O\text{-}(ON{=}CH_2)\}(PH_3)_2$ leads to a dihydride minimum structure with a complete breaking of the H−H bond, while the interaction of the H_2 moiety with the model system $OsCl(NH{=}CHCH{=}CH)(PH_3)_2$ makes the H−H bond breaking/forming process to occur almost without energy barrier.

The different behavior of $OsCl\{\kappa N,\kappa O\text{-}(ON{=}CR_2)\}(P^iPr_3)_2$ and $OsCl\{NH{=}C(Ph)C_6H_4\}(P^iPr_3)_2$ complex fragments toward the H_2 coordination is related to their different singlet−triplet separation. The oximate groups give rise to complex fragments with a singlet−triplet energy promotion smaller than that of the $NH{=}C(Ph)C_6H_4$ ligand, and since the excitation involves the orbitals required for the formation of the M−H bonds, the oximate groups favor the formation of the dihydride form.

Experimental Section

All reactions were carried out with rigorous exclusion of air using Schlenk-tube techniques. Solvents were dried by the usual procedures and distilled under argon prior to use. The starting material $OsH_2Cl_2(P^iPr_3)_2$ (**1**) was prepared by the published method.[11]

In the NMR spectra, chemical shifts are expressed in ppm downfield from Me_4Si (^1H and ^{13}C) and 85% H_3PO_4 (^{31}P). Coupling constants, J, are given in hertz.

Kinetic Analysis. Complete line-shape analyses of the $^1H\{^{31}P\}$ NMR spectra of **2** and **3** were achieved using the program gNMR v3.6 for Macintosh (Cherwell Scientific Publishing Limited). The transverse relaxation time T_2 used was common for the two signals for all temperatures recorded and was obtained from the line width of the exchange-averaged resonance above the fast-exchange limit. The activation parameters $\Delta H^\ddagger$ and $\Delta S^\ddagger$ were calculated by a least-squares fit of $\ln(k/T)$ vs $1/T$ (Eyring equation). Error analysis assumed a 2% error in the rate constant and 1 K in the temperature. Errors were computed by published methods.[23]

Preparation of $OsH_2Cl\{\kappa N,\kappa O\text{-}[ON{=}C(CH_2)_4CH_2]\}(P^iPr_3)_2$ (2). A brown solution of **1** (200 mg, 0.34 mmol) in 15 mL of toluene was treated with cyclohexanone oxime (40 mg, 0,35 mmol) and 0.25 mL (1.8 mmol) of triethylamine. After it was stirred for 20 min at room temperature, the orange suspension was filtered through Kieselguhr and was concentrated to dryness. Addition of methanol yielded a yellow precipitate that was washed (3 × 2 mL) with methanol and dried in vacuo. Yield: 185 mg (82%). Anal. Calcd. for $C_{24}H_{54}NOClOsP_2$: C, 43.65; H, 8.24; N, 2.12. Found: C, 43.27; H, 8.32; N, 2.05. IR (KBr, cm^{-1}): ν(Os−H) 2220 (m), 2157 (s); ν(C=N) 1637 (m). ^1H NMR (300 MHz, toluene-d_8, 253 K): δ 2.66 (m, 2H, $CH_2C{=}N$); 2.26 (m, 6H, PCH); 2.00 (m, 2H, $CH_2C{=}N$); 1.24 (m, 6H, CH_2); 1.30 and 1.16 (both dvt, 36H, $J_{H-H} = 6.6$ Hz, $N = 13.2$ Hz, $PCHCH_3$); −3.22 (br, 1H, OsH); −12.44 (br, 1H, OsH). $^{13}C\{^1H\}$ NMR (75.4 MHz, C_6D_6, 293 K): δ 139.4 (s, C=N); 32.1 and 30.5 (both s, $CH_2C{=}N$); 27.7, 26.0 and 25.4 (all s, CH_2); 25.0 (vt, $N = 24$ Hz, PCH); 19.8 and 18.1 (both s, $PCHCH_3$). $^{31}P\{^1H\}$ NMR (121.4 MHz, C_6D_6, 293 K): δ 12.3 (s). MS (FAB$^+$): m/z 659 (M^+) and 623 ($M^+ - Cl$).

Table 4. Crystal Data and Data Collection and Refinement for $OsH_2Cl\{\kappa N,\kappa O\text{-}[ON{=}C(CH_2)_4CH_2]\}(P^iPr_3)_2$

formula	$C_{24}H_{54}ClNOOsP_2$
mol wt	660.27
color, habit	orange
space group	monoclinic, $P2_1/c$
a, Å	14.8951(9)
b, Å	9.5382(6)
c, Å	20.8395(12)
β, deg	104.369(1)
V, Å^3	2868.1(3)
Z	4
D(calcd), g cm^{-3}	1.529
μ, mm^{-1}	4.666
scan type	ω scans at different φ values
θ range, deg	$2 \le \theta \le 28.4$
temp, K	153.0(2)
no. of data collected	10 239
no. of unique data	5463 ($R_{int} = 0.0343$)
no. of params refined	379
R1^a ($F^2 > 2\sigma(F^2)$)	0.0325
wR2^b (all data)	0.0759
S^c (all data)	1.056

[a] $R1(F) = \sum||F_o| - |F_c||/\sum|F_o|$. [b] $wR2(F^2) = [\sum[w(F_o^2 - F_c^2)^2]/\sum[w(F_o^2)^2]]^{1/2}$; $w^{-1} = [\sigma^2(F_o^2) + (0.0341P)^2 + 1.9443P]$, where $P = [\max(F_o^2,0) + 2F_c^2)]/3$. [c] $S = [\sum[w(F_o^2 - F_c^2)^2]/(n - p)]^{1/2}$, where n is the number of reflections and p the number of refined parameters.

Preparation of $OsClH_2\{\kappa N,\kappa O\text{-}[ON{=}C(CH_3)_2]\}(P^iPr_3)_2$ (3). This complex was prepared as described for **2**, by starting from **1** (200 mg, 0.34 mmol) with 25 mg (0.34 mmol) of acetone oxime and 0.25 mL (1.8 mmol) of triethylamine. An orange microcrystalline solid was obtained. Yield: 182 mg (86%). Anal. Calcd for $C_{21}H_{50}NOClOsP_2$: C, 40.66; H, 8.12; N, 2.25. Found: C, 40.43; H, 7.82; N, 2.14. IR (KBr, cm^{-1}): ν(Os−H) 2189 (m), 2165 (s); ν(C=N) 1642 (m). ^1H NMR (300 MHz, toluene-d_8, 243 K): δ 2.20 (m, 6H, PCH); 1.95 and 1.47 (both s, 6H, $CH_3C{=}N$); 1.26 and 1.12 (both dvt, 36H, $J_{H-H} = 6.3$ Hz, $N = 12.9$ Hz, $PCHCH_3$); −3.24 (br, 1H, OsH); −12.6 (br, 1H, OsH). $^{13}C\{^1H\}$ NMR (75.4 MHz, C_6D_6, 293 K): δ 133.9 (s, C=N); 24.7 (vt, $N = 23.7$ Hz, PCH); 21.2 and 19.2 (both s, $CH_3C{=}N$); 19.7 and 18.6 (both s, $PCHCH_3$). $^{31}P\{^1H\}$ NMR (121.4 MHz, C_6D_6, 293 K): δ 12.4 (s). MS (FAB$^+$): $m/z = 586$ (M^+).

X-ray Structure Analysis of $OsH_2Cl\{\kappa N,\kappa O\text{-}[ON{=}C(CH_2)_4CH_2]\}(P^iPr_3)_2$ (2). Crystals suitable for the X-ray diffraction study were obtained by cooling at 258 K a saturated solution of **2** in diethyl ether. A summary of crystal data and refinement parameters is reported in Table 4. The orange, prismatic crystal, of approximate dimensions 0.08 × 0.06 × 0.01 mm, was glued on a glass fiber and mounted on a Siemens-CCD diffractometer (sealed tube 2.4 kW, $\lambda = 0.710\,73$ Å). A total of 10 239 data were collected via runs of 0.3° ω scans at different φ values, over a θ range of 2.5−28.4°. All data were corrected for absorption using the SADABS program.[24] The structure was solved by direct methods[25] and conventional Fourier techniques and refined by full-matrix least squares on F^2 (SHELXL97).[25] Anisotropic parameters were used in the last cycles of refinement for all non-hydrogen atoms. Hydrogen atoms were included in observed positions and refined freely or refined riding on their respective carbon atoms. Atomic scattering factors, corrected for anomalous dispersion, were implemented by the program. The refinement converge to $R1 = 0.0325$ ($F^2 > 2\sigma(F^2)$) and $wR2 = 0.0759$ (all data), with weighting parameters $x = 0.0341$ and $y = 1.9443$.

---

(23) Morse, P. M.; Spencer, M. D.; Wilson, S. R.; Girolami, G. S. *Organometallics* **1994**, *13*, 1646 and references therein.

(24) SADABS program: Sheldrick, G. *SADABS User Guide*; Institüt für Anorganische Chemie der Universität: Göttingen, Germany, 1995.

(25) Sheldrick, G. SHELXL-97: Program for Crystal Structure Refinement; Institüt für Anorganische Chemie der Universität, Göttingen, Germany, 1997.

Computational Details. Calculations were performed with the GAUSSIAN94 series of programs.[26] Geometry optimizations were carried out using the density functional theory (DFT)[27] with the B3LYP functional.[28] An effective core potential operator was used to represent the innermost electrons of the osmium atom.[29] The basis set for the metal was that associated with the pseudopotential,[29] with a standard valence double-ζ LANL2DZ contraction.[26] The basis set for the hydrogen atoms directly attached to the metal was double-ζ supplemented with a polarization p shell.[30a,b] A 6-31G(d) basis was used for Cl, P, N, and O atoms, as well as for the C coordinated to the metal in complex **5**.[30c] The rest of the atoms were described using a 6-31G basis set.[30a]

To obtain accurate estimations for the oxidative addition energy profiles, the geometries were optimized at the B3LYP level and energies recalculated using coupled-cluster theory with single, double, and a noniterative estimation of triple excitations (CCSD(T)//B3LYP).[31] The metal−dihydrogen and metal−hydride dissociation energies and the singlet/triplet energy differences in the fragments were also calculated at the CCSD(T)//B3LYP level.

Acknowledgment. Financial support from the DGES of Spain (Projects PB95-0639-C02-01 and PB95-0806) is acknowledged. R.C. thanks the Ministerio de Educación y Ciencia for a grant. J.T. acknowledges also the "Direcció General de Recerca de la Generalitat de Catalunya" for a grant. The use of computational facilities of the Centre de Supercomputació i Comunicacions de Catalunya is gratefully appreciated as well.

Supporting Information Available: Tables of atomic coordinates, anisotropic and isotropic thermal parameters, experimental details of the X-ray study, and bond distances and angles. This material is available free of charge via the Internet at http://pubs.acs.org.

OM9904192

---

(26) Frisch, M. J.; Trucks, G. W.; Schlegel, H. B.; Gill, P. M. W.; Johnson, B. G.; Robb, M. A.; Cheeseman, J. R.; Keith, T. A.; Petersson, G. A.; Montgomery, J. A.; Raghavachari, K.; Al-Laham, M. A.; Zakrzewski, V. G.; Ortiz, J. V.; Foresman, J. B.; Cioslowski, J.; Stefanov, B. B.; Nanayakkara, A.; Challacombe, M.; Peng, C. Y.; Ayala, P. Y.; Chen, W.; Wong, M. W.; Andres, J. L.; Replogle, E. S.; Gomperts, R.; Martin, R. L.; Fox, D. J.; Binkley, J. S.; Defrees, D. J.; Baker, J.; Stewart, J. P.; Head-Gordon, M.; Gonzalez, C.; Pople, J. A. *Gaussian 94*; Gaussian Inc., Pittsburgh, PA, 1995.

(27) Parr, R. G.; Yang, W. *Density-Functional Theory of Atoms and Molecules*; Oxford University Press: Oxford, U.K., 1989.

(28) (a) Lee, C.; Yang, W.; Parr, R. G. *Phys. Rev. B* **1988**, *37*, 785. (b) Becke, A. D. *J. Chem. Phys.* **1993**, *98*, 5648. (c) Stephens, P. J.; Devlin, F. J.; Chabalowski, C. F.; Frisch, M. J. *J. Phys. Chem.* **1994**, *98*, 11623.

(29) Hay, P. J.; Wadt, W. R. *J. Chem. Phys.* **1985**, *82*, 299.

(30) (a) Hehre, W. J.; Ditchfield, R.; Pople, J. A. *J. Chem. Phys.* **1972**, *56*, 2257. (b) Hariharan, P. C.; Pople, J. A. *Theor. Chim. Acta* **1973**, *28*, 213. (c) Francl, M. M.; Pietro, W. J.; Hehre, W. J.; Binkley, J. S.; Gordon, M. S.; DeFrees, D. J.; Pople, J. A. *J. Chem. Phys.* **1982**, *77*, 3654.

(31) (a) Bartlett, R. J. *J. Phys. Chem.* **1989**, *93*, 1697. (b) Bartlett, R. J.; Watts, J. D.; Kucharski, S. A.; Noga, J. *Chem. Phys. Lett.* **1990**, *165*, 513.